Effects of Aromatic Residues at the Ends of Transmembrane α-Helices on Helix Interactions with Lipid Bilayers[†]

Sanjay Mall, Robert Broadbridge, Ram P. Sharma, Anthony G. Lee, and J. Malcolm East*

Division of Biochemistry and Molecular Biology, School of Biological Sciences, University of Southampton, Southampton, SO16 7PX, U.K.

Received September 22, 1999; Revised Manuscript Received December 3, 1999

ABSTRACT: We have studied the effects of aromatic residues at the ends of peptides of the type Ac-KKGL$_n$WL$_m$KKA-amide on their interactions with lipid bilayers as a function of lipid fatty acyl chain length, physical phase, and charge. Peptide Ac-KKGFL$_6$WL$_8$FKKA-amide (F$_2$L$_{14}$) incorporated into bilayers of phosphatidylcholines containing monounsaturated fatty acyl chains of lengths C14−C24 at a peptide: lipid molar ratio of 1:100 in contrast to Ac-KKGL$_7$WL$_9$KKA-amide (L$_{16}$) which did not incorporate at all into dierucoylphosphatidylcholine [di(C24:1)PC]; Ac-KKGYL$_6$WL$_8$YKKA-amide (Y$_2$L$_{14}$) incorporated partly into di(C24:1)PC. Lipid-binding constants relative to that for dioleoylphosphatidylcholine (C18:1)PC were obtained using a fluorescence quenching method. For Y$_2$L$_{14}$ and F$_2$L$_{14}$, relative lipid-binding constants increased with increasing fatty acyl chain length from C14 to C24; strongest binding did not occur at the point where the hydrophobic length of the peptide equalled the hydrophobic thickness of the bilayer. For Ac-KKGYL$_9$WL$_{11}$YKKA-amide (Y$_2$L$_{20}$), increasing chain length from C18 to C24 had little effect on relative binding constants. Anionic phospholipids bound more strongly than zwitterionic phospholipids to Y$_2$L$_{14}$ and Y$_2$L$_{20}$ but effects of charge were relatively small. In two phase (gel and liquid crystalline) mixtures, all the peptides partitioned more strongly into liquid crystalline than gel phase; effects were independent of the structure of the peptide or of the lipid (dipalmitoylphosphatidylcholine or bovine brain sphingomyelin). Addition of cholesterol had little effect on incorporation of the peptides into lipid bilayers. It is concluded that the presence of aromatic residues at the ends of transmembrane α-helices effectively buffers them against changes in bilayer thickness caused either by an increase in the chain length of the phospholipid or by the presence of cholesterol.

The membrane-spanning regions of most intrinsic membrane proteins consist of one or more hydrophobic, transmembrane α-helices. For some membrane proteins, often referred to as stalked proteins, these helices serve merely to anchor the protein in the membrane. However, for others, the transmembrane α-helices are important for the function of the protein, and for such proteins, the organization and packing of α-helices in the membrane will be an important feature of the structure of the protein. One factor affecting the organization of transmembrane α-helices is their interaction with the surrounding phospholipid bilayer. In particular, the hydrophobic thickness of the lipid bilayer must be matched to the hydrophobic length of a transmembrane α-helix because the energetic cost of exposing either fatty acyl chains or hydrophobic amino acids to water is high. When the hydrophobic thickness of the bilayer exactly matches the hydrophobic length of the α-helix, the α-helix can simply span the bilayer with its long axis parallel to the bilayer normal. This type of organization has been confirmed for simple peptides of the type Ac-K$_2$GL$_n$K$_2$A-amide containing a long stretch of Leu residues located between two pairs of Lys residues; the Lys residues in these peptides serve to anchor the peptide across the membrane and to minimize the chance of peptide aggregation within the membrane (*1*, *2*). Peptides whose hydrophobic lengths are greater than the hydrophobic thickness of the bilayer will also incorporate across a lipid bilayer, hydrophobic matching presumably being achieved by tilting the long axis of the peptide relative to the bilayer normal (*3*−*6*). However, when the hydrophobic length of the peptide is much less than the hydrophobic thickness of the bilayer, the peptide cannot adopt an orientation spanning the lipid bilayer and thus either binds to the surface of the bilayer or forms a separate aggregate in water (*3*−*5*).

In ion channels and transporters where the transmembrane α-helices define the pathway for ion movement across the membrane, the correct angle of tilt of the helices is likely to be important for function. For example, in the potassium channel KcsA, the two helices per monomeric unit are each tilted across the membrane at an angle of about 15° with respect to the bilayer surface (*7*). Changing the thickness of the lipid bilayer could change the angle of tilt of the helices, the tilt angle increasing or decreasing as, respectively, the bilayer thins or thickens. The importance of bilayer thickness has been shown in studies of the activity of the Ca^{2+}-ATPase; ATPase activity was found to be highest in bilayers of dioleoylphosphatidylcholine [di(C18:1)PC],[1] with lower activities in bilayers of longer or shorter chain phospholipids (*8*−*11*).

[†] We thank the BBSRC for financial support.

* To whom correspondence should be addressed. Phone: 44 (0) 2380 594222. Fax: 44 (0) 2380 594459. E-mail: jme1@soton.ac.uk.

10.1021/bi992205u CCC: $19.00
Published on Web 01/29/2000

Analysis of the compositions of the predicted transmembrane domains of a large number of bitopic membrane proteins showed that while the most common residue was Leu, aromatic residues are commonly found at the ends of the helices (*12*). This predicted nonrandom distribution is also observed in crystal structures of membrane proteins. For example, in the photosynthetic reaction center, the majority of the Trp residues is found near the periplasmic side of the protein near the ends of the helices where they can form hydrogen bonds with suitable groups in the lipids (*13*). Similarly, in the crystal structure of the potassium channel KcsA, aromatic residues are found clustered at the ends of the trans-membrane α-helices (*7*). Measurements of binding of peptides at the lipid−water interface have confirmed the preference of aromatic residues for the lipid−water interface (*14*). It has been suggested that the role of aromatic residues at the ends of transmembrane α-helices is to act as "floats" at the interface, serving to fix the helix within the lipid bilayer with the polar groups facing the water and the nonpolar aromatic regions penetrating into the hydrocarbon region.

Interactions between lipid bilayers and Trp-containing peptides of the type Ac-$K_2GL_mWL_nK_2A$-amide (L_{m+n}) can be studied using the Trp residue as a fluorescence reporter group (*3*). Introduction of a Trp residue into the middle of the peptide has been shown not to affect the transmembrane orientation adopted by the peptide (*15*). A fluorescence quenching method has been used to characterize selectivity in the interaction between the peptides and particular lipids (*16*). The peptide is incorporated into bilayers containing the brominated phospholipid dibromostearoylphosphatidylcholine [di(Br_2C18:0)PC]; di(Br_2C18:0)PC behaves much like a conventional phospholipid with unsaturated fatty acyl chains because the bulky bromine atoms have similar effects on lipid packing as a cis double bond (*16*). In mixtures of brominated and nonbrominated phospholipids, the degree of quenching of the fluorescence of the tryptophan residue in the peptide is related to the fraction of the surrounding phospholipids which are brominated and, thus, to the strength of binding of the nonbrominated lipid to the peptide. Here, we show that the presence of Phe and Tyr residues at the ends of transmembrane α-helices have marked effects on interactions of the peptides with lipid bilayers of different thicknesses, charges, and physical phases.

MATERIALS AND METHODS

Materials and General Procedures. Dimyristoleoylphosphatidylcholine [di(C14:1)PC], dipalmitoleoylphosphatidylcholine [di(C16:1)PC], dioleoylphosphatidylcholine [di(C18:1)P], dieicosenoylphosphatidylcholine [di(C20:1)P], dierucoylphosphatidylcholine [di(C22:1)PC], dinervonylphosphatidylcholine [di(C24:1)PC], dioleoylphosphatodylserine [di(C18:1)PS], and dioleoylphosphatidic acid [di(C18:1)PA] were obtained from Avanti Polar Lipids; dipalmitoylphosphatidylcholine [di(C16:0)PC] and bovine brain sphingomyelin were from Sigma. Di(C18:1)PC was brominated to give di(Br_2C18:0)PC as described in East and Lee (*16*), and the same procedure was used to brominate di(C18:1)PS to dibromostearoylphosphatidylserine [di(Br_2C18:0)PS] and di(C18:1)PA to dibromostearoylphosphatidic acid [di(Br_2C18:0)PA]. Peptides Ac-$KKGL_7WL_9KKA$-amide (L_{16}), Ac-$KKGL_{10}WL_{12}KKA$-amide (L_{22}), Ac-$KKGYL_6WL_8YKKA$-amide (Y_2L_{14}), Ac-$KKGYL_9WL_{11}YKKA$-amide (Y_2L_{20}), and Ac-$KKGFL_6WL_8FKKA$-amide (F_2L_{14}) were synthesized using t-Boc chemistry (*17*), and purity was confirmed using electrospray mass spectroscopy.

Peptides (20 nmol) were incorporated into phospholipid bilayers by mixing peptide and lipid at a molar ratio of peptide to phospholipid of 1:100 in methanol. Solvent was removed under vacuum, buffer (400 μL) was added, and the sample was placed in a bath sonicator for a few minutes to disperse the lipid−peptide mixture into the buffer, giving a preparation of multilamellar vesicles (MLVs). Aliquots (100 μL) of the sample were diluted into buffer (2.5 mL; 20 mM Hepes and 1 mM EGTA, pH 7.2), and fluorescence intensities were recorded at 25 °C using an SLM-Aminco 8000C fluorimeter, with an excitation wavelength of 280 nm.

To obtain accurate values for wavelengths of maximum fluorescence emission intensity (λ_{max}), fluorescence spectra were fitted to skewed Gaussian curves (*18*) over the wavelength range $F > 0.25F_{max}$:

$$F = F_{max} \exp\{-(\ln 2)[\ln(1 + 2b(\lambda - \lambda_{max})/\omega_\lambda)/b]^2\} \quad (1)$$

where F and F_{max} are the fluorescence intensities at wavelengths λ and λ_{max}, respectively, b is the skew parameter, and ω_λ is the peak width at half-height.

Quenching Analysis. The fluorescence lifetime for tryptophan is considerably less than the time for two lipids to exchange position in a bilayer, so that contact quenching of Trp fluorescence by a brominated phospholipid can be considered to be a static phenomenon (*19*). Quenching can then be analyzed in either of two ways. The first is a lattice model of quenching (*16*, *20*). The degree of quenching in the lattice model is proportional to the probability that a brominated lipid occupies a lattice site close enough to the peptide to cause quenching. For a random distribution of lipids (no selectivity in binding to the peptide), the probability that any lattice site is not occupied by a brominated lipid is $1 - x_{Br}$ where x_{Br} is the mole fraction of brominated lipid in the bilayer. The probability that any particular peptide will give rise to fluorescence is proportional to the probability that none of the n lattice sites close enough to the peptide to cause quenching is occupied by a brominated lipid. Thus,

$$F/F_o = F_{min} + (F_o - F_{min})(1 - x_{Br})^n \quad (2)$$

where F_o and F_{min} are the fluorescence intensities for the peptide in nonbrominated and brominated lipid, respectively, and F is the fluorescence intensity in the phospholipid mixture when the mole fraction of brominated lipid is x_{Br}. In mixtures of brominated and nonbrominated phospholipids, where there is selectivity of binding to the peptide, eq 2 can be rewritten as

[1] Abbreviations: di(C14:1)PC, dimyristoleoylphosphatidylcholine; di(C16:0)PC, dipalmitoylphosphatidylcholine; di(C16:1)PC, dipalmitoleoylphosphatidylcholine; di(C18:1)PC, dioleoylphosphatidylcholine; di(C20:1)PC, dieicosenoylphosphatidylcholine; di(C22:1)PC, dierucoylphosphatidylcholine; di(C24:1)PC, dinervonylphosphatidylcholine; di(C18:1)PA, dioleoylphosphatidic acid; di(C18:1)PS, dioleoylphosphatodylserine; di(Br_2C18:0)PC, dibromostearoylphosphatidylcholine; di(Br_2C18:0)PA, dibromostearoylphosphatidic acid; di(Br_2C18:0)PS, dibromostearoylphosphatidylserine; L_{16}, Ac-$KKGL_7WL_9KKA$-amide; L_{22}, Ac-$KKGL_{10}WL_{12}KKA$-amide; Y_2L_{14}, Ac-$KKGYL_6WL_8YKKA$-amide; Y_2L_{20}, Ac-$KKGYL_9WL_{11}YKKA$-amide; F_2L_{14}, Ac-$KKGFL_6WL_8FKKA$-amide; MLV, multilamellar vesicles.

$$F/F_o = F_{min} + (F_o - F_{min})(1 - f_{Br})^n \quad (3)$$

where f_{Br} is the fraction of sites at the lipid−protein interface occupied by brominated lipid. The fraction of sites occupied by brominated lipid is related to x_{Br} by

$$f_{Br} = x_{Br}/(x_{Br} + K[1 - x_{Br}]) \quad (4)$$

where K is the relative binding constant of the nonbrominated phospholipid with respect to the brominated phospholipid.

An alternative description of quenching is the sphere of action model (*21*). This assumes the existence of a sphere of volume around a fluorophore within which a quencher will cause quenching with a probability of unity. Adapting this model to the two-dimensional case of a biological membrane gives

$$F/F_o = F_{min} + (F_o - F_{min})\exp(-\pi r^2 C_{Br}) \quad (5)$$

where πr^2 is the area of the quenching circle around each tryptophan and C_{Br} is the concentration of brominated lipid in units of molecules per unit area. The distribution of nonbrominated lipid between the quenching circle and the bulk lipid can be described by a constant K (the partition coefficient for nonbrominated lipid relative to brominated lipid) so that in the case of selective interaction with the peptide eq 5 becomes

$$F/F_o = F_{min} + (F_o - F_{min})\exp(-\pi r^2 C_{Br}/K) \quad (6)$$

Data were fitted to all equations using the Marquardt−Levenberg algorithm in SigmaPlot.

RESULTS

Fluorescence Properties of the Peptides as a Function of Lipid Chain Length. The Trp-containing peptides were incorporated into bilayers of lipid by mixing peptide and lipid in organic solvent, removing the solvent, and then hydrating the mixture. In a previous publication, we showed that the intensity of the fluorescence of the Trp residue in the peptides could be used to determine whether the peptide was incorporated into the lipid bilayer (*3*). Peptide in water had a very low fluorescence intensity, attributed to the formation of aggregates in water, whereas peptide incorporated into the lipid bilayer gave high fluorescence intensity, centered at about 320−330 nm, characteristic of a Trp residue in a hydrophobic environment (*3*). We also showed that whereas the peptide L_{22} incorporated into bilayers of all phosphatidylcholines with monounsaturated fatty acyl chains of lengths between C14 and C24, the peptide L_{16} only incorporated fully into bilayers when the fatty acyl chain length was C20 or less (*3*).

Peptide F_2L_{14}, unlike peptide L_{16}, incorporated into all phosphatidylcholines containing monounsaturated fatty acyl chains with lengths between C14 and C24 (Figure 1A). However, although peptide Y_2L_{14} incorporated fully into bilayers of phosphatidylcholine with chain lengths from C14 to C22, the fluorescence intensity in di(C24:1)PC was less than that in the shorter chain phospholipids (Figure 1B). The fluorescence intensity of Y_2L_{14} in di(C24:1)PC was seen to increase with increasing molar ratio of lipid:peptide and at 400:1 was very similar to the intensity observed in di(C18:1)PC at a molar ratio of lipid:peptide of 100:1; incorporation of peptides into di(C18:1)PC was complete by a molar ratio of lipid:peptide of about 15:1 (data not shown). Thus Y_2L_{14} incorporates only partially into bilayers of di(C24:1)PC, an equilibrium being established between nonfluorescent aggregates in water and bilayer-incorporated peptide. The longer peptide Y_2L_{20} was found to incorporate fully into bilayers of phosphatidylcholines with chain lengths between C14 and C24 (data not shown).

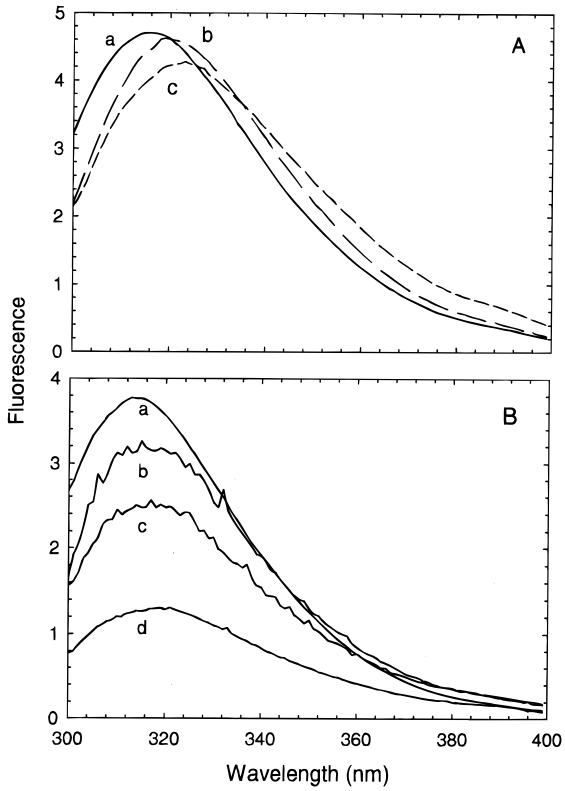

FIGURE 1: Fluorescence emission spectra. (A) F_2L_{14} in bilayers of (a) di(C18:1)PC; (b) di(C14:1)PC; (c) di(C24:1)PC. For all samples the molar ratio of lipid:peptide was 100:1. (B). Y_2L_{14} in bilayers of di(C18:1)PC at a molar ratio of lipid:peptide of 100:1 (a) and in bilayers of di(C24:1)PC at molar ratios of lipid:peptide of (b) 400:1; (c) 100:1; (d) 50:1. For all spectra, the concentration of peptide was 0.02 μM.

Fluorescence emission maxima for Trp are environmentally sensitive, generally shifting to longer wavelength with increasing solvent polarity, although effects of environmental mobility can also be important (*21*). Ren et al. (*4*, *5*) have shown that the fluorescence emission maxima of peptides of the type Ac-$K_2GL_mWL_nK_2A$-amide incorporated into lipid bilayers are sensitive to bilayer thickness. A similar dependence is seen for peptides containing aromatic residues at the ends of the helices (Figure 2). Minimum values for λ_{max} for Y_2L_{14} and F_2L_{14} are observed at a chain length of about C18, compared to C22 for Y_2L_{20}; for L_{16} and L_{22}, minimum values for λ_{max} are observed at about C20 for both peptides. Values for λ_{max} are similar for L_{16} and F_2L_{14}, but λ_{max} values are smaller for Y_2L_{14} than for L_{16} and also smaller for Y_2L_{20} than for L_{22}; it is not clear whether this reflects a small change in the fluorescence properties of the peptides or a slightly more nonpolar environment for the Trp residue in the Tyr-containing peptides. Changes in λ_{max} are small, and values for λ_{max} do not approach the value of about 350 nm typical for a Trp residue exposed to water (*21*). Thus, all

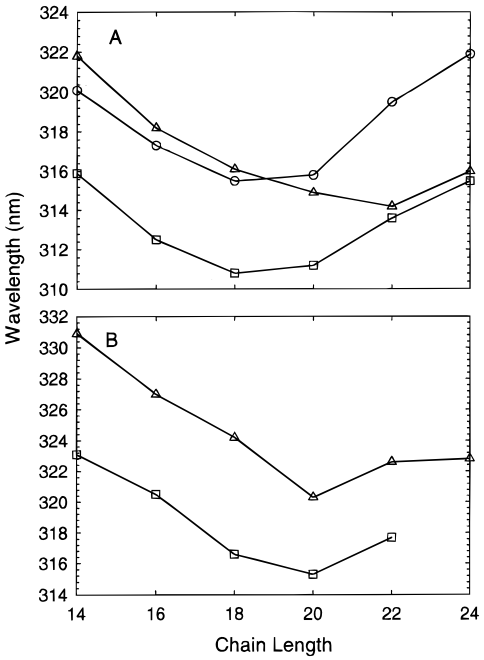

FIGURE 2: The effect of fatty acyl chain length on the λ_{max} for peptides in bilayers of phosphatidylcholine. The fatty acyl chain lengths are plotted against λ_{max} for (A) (□) Y_2L_{14}; (○) F_2L_{14}; (△) Y_2L_{20}; and (B) (□) L_{16}; (△) L_{22}. Samples contained 0.02 μM peptide in 2 μM lipid.

peptides are incorporated into the lipid bilayers with the Trp residue in a hydrophobic environment, consistent with the peptide spanning the lipid bilayer. For peptide Y_2L_{14} in di(C24:1)PC, the value of λ_{max} shifts only from 317.7 to 315.6 nm with increasing molar ratio of lipid:peptide from 50:1 to 400:1, despite the 2.5-fold increase in fluorescence intensity (Figure 1B). This suggests that the peptide simply equilibrates between an almost nonfluorescent state in water and a fluorescent state spanning the lipid bilayer with the state of the peptide that is incorporated into the bilayer being almost independent of the total molar ratio of lipid:peptide.

Quenching of Fluorescence by Brominated Phospholipids. Incorporation of the peptides into bilayers of di(Br_2C18:0)PC leads to quenching of Trp fluorescence (Figure 3). The fluorescence intensities recorded in mixtures of di(C18:1)PC and di(Br_2C18:0)PC decrease with increasing content of di(Br_2C18:0)PC; the data fit to eq 2 with a value for *n*, the number of "sites" around the peptide, of 2.8 for F_2L_{14} and Y_2L_{14} and 2.4 for Y_2L_{20}, comparable to the values of *n* of 2.7 and 2.3 determined previously for L_{16} and L_{22}, respectively (*3*). The value of *n* describing the quenching of Trp fluorescence in the Ca^{2+}-ATPase by brominated phospholipids is 1.6 (*16*), suggesting that the Trp residues in the peptides are more exposed to the surrounding lipid than those in a membrane protein with multitransmembrane α-helices.

As shown in Figure 3, panels A and B, fluorescence quenching curves for F_2L_{14} and Y_2F_{14} in mixtures of di(Br_2-C18:0)PC and (C14:1)PC show more fluorescence quenching at intermediate mole fractions of di(Br_2C18:0)PC than seen in mixtures with di(C18:1)PC, whereas less fluorescence quenching is seen at intermediate mole fractions in mixtures with di(C24:1)PC. These results show that the lipid−peptide interaction is chain length dependent. Analysis of the data in terms of eqs 2−4 gives the binding constant for the lipid,

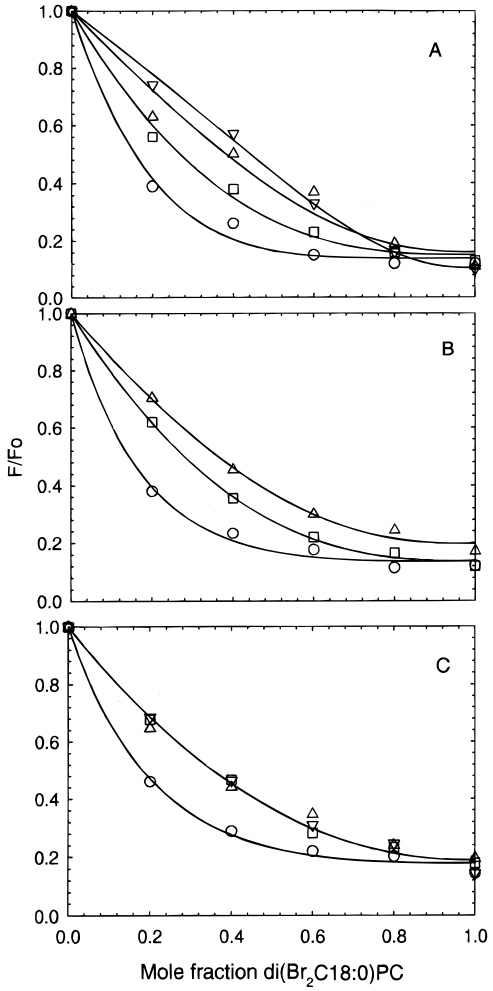

FIGURE 3: Fluorescence intensities in mixtures of di(Br_2C18:0)PC and nonbrominated phosphatidylcholine. F_2L_{14} (A), Y_2L_{14} (B), or Y_2L_{20} (C) were incorporated into mixtures of di(Br_2C18:0)PC with di(C14:1)PC (○), di(C18:1)PC (□), di(C22:1)PC (△), or di(C24:1)PC (▽), at a molar ratio of lipid:peptide of 100:1. Fluorescence intensities are expressed as a fraction of that for the peptide in 100% nonbrominated lipid. The solid lines show best fits of the data to eqs 2−4 with the relative binding constants given in Table 1. In panel C, fits to data for di(C18:1)PC, di(C22:1)PC, and di(C24:1)PC are almost identical; for clarity only, that for di(C18:1)PC is shown.

relative to that for di(C18:1)PC; the results listed in Table 1 show that the longer chain phospholipids bind more strongly to F_2L_{14} and Y_2L_{14} than short-chain phospholipids. Quenching for the longer peptide Y_2L_{20} is markedly less dependent on fatty acyl chain length, with essentially equal binding to phosphatidylcholines with chain lengths between C18 and C24 (Figure 3C, Table 1).

The data can also be interpreted in terms of a quenching circle model, in which any brominated phospholipid molecule within a quenching circle around the peptide results in quenching. The data for F_2L_{14} and Y_2L_{14} in mixtures of di(Br_2C18:0)PC and (C18:1)PC fit to eq 5 with fits as good as to eq 2, with a circle radius *r* of 8.3 ± 2.0 Å, calculated assuming an area occupied by a lipid in the bilayer surface of 70 Å^2; for Y_2L_{20}, the data fit to a radius *r* of 7.0 ± 1.9 Å (data not shown). Data in mixtures of di(Br_2C18:0)PC and other phosphatidylcholines can then be fitted to eq 6, using these values of *r*, to give the relative binding constants also listed in Table 1.

Table 1: Relative Lipid Binding Constants

lipid	d (Å)[a]	relative binding constant[b]			relative partition coefficient[c]		
		Y_2L_{14}	F_2L_{14}	Y_2L_{20}	Y_2L_{14}	F_2L_{14}	Y_2L_{20}
di(C14:1)PC	22.8	0.46 ± 0.05	0.50 ± 0.06	0.47 ± 0.04	0.53 ± 0.04	0.56 ± 0.02	0.44 ± 0.03
di(C16:1)PC	26.1	0.74 ± 0.09	0.83 ± 0.08	0.45 ± 0.05	0.80 ± 0.07	0.86 ± 0.07	0.43 ± 0.03
di(C18:1)PC	29.8	1	1	1	1	1	1
di(C20:1)PC	33.3	1.02 ± 0.24	1.16 ± 0.12	1.22 ± 0.1	1.10 ± 0.21	1.22 ± 0.06	0.95 ± 0.20
di(C22:1)PC	36.8	1.37 ± 0.09	1.62 ± 0.36	0.96 ± 0.1	1.49 ± 0.14	1.60 ± 0.37	0.87 ± 0.06
di(C24:1)PC	40.3		2.33 ± 0.16	1.19 ± 0.12		1.68 ± 0.06	1.13 ± 0.08

[a] Hydrophobic thickness of the bilayer calculated from $d = 1.75(n - 1)$, where n is the number of carbon atoms in the fatty acyl chain (*38*, *39*). [b] Binding constant relative to that for di(C18:1)PC, calculated using eqs 2−4 with values of n of 2.8 for Y_2L_{14} and F_2L_{14} and 2.4 for Y_2L_{20}. [c] Relative partition coefficient between the quenching circle around the peptide and the bulk lipid, calculated using eq 6 with values of r of 8.3 Å for Y_2L_{14} and F_2L_{14} and 7.0 Å for Y_2L_{20}.

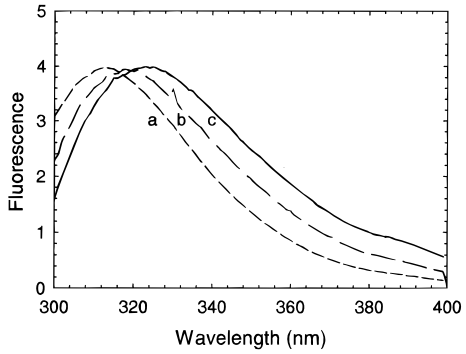

FIGURE 4: Effects of gel phase phospholipid. Fluorescence emission spectra are shown for Y_2L_{14} in di(C16:1)PC (a) and di(C16:0)PC in the gel phase (b) and for L_{16} in di(C16:0)PC in the gel phase (c), at 25 °C. The molar ratio of phospholipid to protein was 100:1.

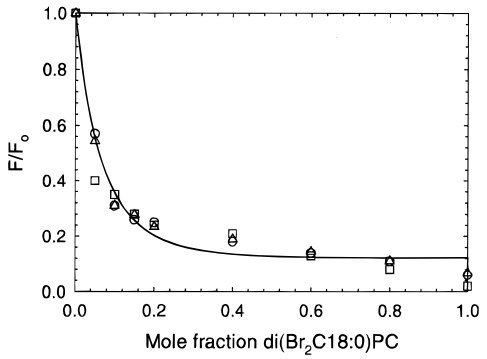

FIGURE 5: Fluorescence intensities in mixtures of di(Br_2C18:0)PC and gel phase lipid. Fluorescence intensities are shown for L_{16} (○) and Y_2L_{14} (△) in mixtures of di(Br_2C18:0)PC and di(C16:0)PC and for L_{16} in mixtures of di(Br_2C18:0)PC and sphingomyelin (□), at 25 °C. The lines show fits to eqs 2−4 with the relative binding constants given in the text. The molar ratio of phospholipid to protein was 100:1

Effects of Gel Phase Lipid. Figure 4 compares fluorescence emission spectra for Y_2L_{14} in bilayers of di(C16:0)PC in the gel phase at 25 °C with the spectrum in liquid crystalline phase di(C16:1)PC. The spectrum in gel phase lipid is shifted about 5 nm to longer wavelength compared to that in liquid crystalline phase lipid, but the value for λ_{max} (317.8 nm) and the fluorescence intensity [equal to that in di(C16:1)PC] show that the peptide is fully incorporated into the gel phase bilayer. Peptide L_{16} is also fully incorporated into gel phase di(C16:0)PC (Figure 4), as are peptides F_2L_{14} and Y_2L_{20} (data not shown).

Quenching profiles in mixtures of di(Br_2C18:0)PC and di-(C16:0)PC are shown in Figure 5, and the very marked quenching at low mole fractions of di(Br_2C18:0)PC show that the peptides are excluded from gel phase di(C16:0)PC in these mixtures. The data fit to a relative binding constant of 0.14 ± 0.08 for L_{16} and 0.17 ± 0.02 for Y_2L_{14}. Very similar quenching profiles are observed for F_2L_{14}, L_{22} and Y_2L_{20}, showing that these peptides are also excluded from gel phase lipid (data not shown).

The quenching profile for L_{16} in mixtures of di(Br_2C18:0)PC and bovine brain sphingomyelin is also shown in Figure 5; the experimental data fit to a relative binding constant for sphingomyelin of 0.14 ± 0.03. The phase transition temperature for bovine brain sphingomyelin is ca. 35 °C (*22*) so that this again shows exclusion of the peptide from gel phase lipid.

Effects of Cholesterol. Addition of cholesterol up to a molar ratio of cholesterol:phospholipid of 1:1 had very little effect on the Trp fluorescence intensity for L_{16} in di(C14:1)PC but in di(C18:1)PC resulted in a marked decrease in intensity beyond a mole ratio of 0.6, as reported previously (*3*) (Figure 6). In contrast, addition of cholesterol up to a 1:1 molar ratio had very little effect on the fluorescence intensities for F_2L_{14} or Y_2L_{14} in di(C18:1)PC or for F_2L_{14} in di(C24:1)PC (Figure 6). Effects of cholesterol on values of λ_{max} were very small. For L_{16} in di(C18:1)PC, the value of λ_{max} shifted from 316.6 to 316.8 nm on addition of cholesterol at a molar ratio of 1:1, despite the 60% decrease in fluorescence intensity. This is consistent with simple equilibration of the peptide between an almost nonfluorescent state in water and a fluorescent state spanning the lipid bilayer, partitioning into the bilayer being reduced in the presence of cholesterol.

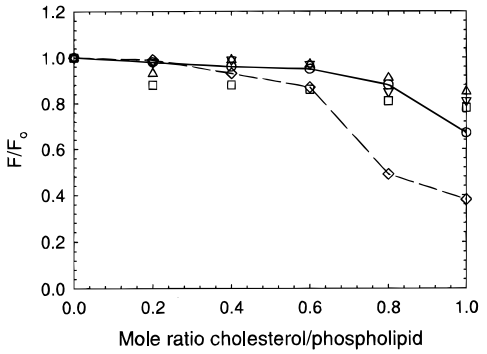

FIGURE 6: Effects of cholesterol. The fluorescence intensity was recorded as a function of the mole ratio of cholesterol:phospholipid for L_{16} in di(C14:1)PC (○) and di(C18:1)PC (◇), Y_2L_{14} in di(C18:1)PC (▽) and F_2L_{14} in di(C18:1)PC (△) and di(C24:1)PC (□). The molar ratio of phospholipid to protein was 100:1.

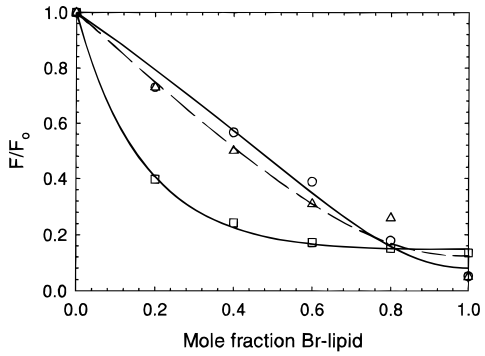

FIGURE 7: Fluorescence intensities in mixtures of phosphatidic acid and phosphatidylcholine. Y_2L_{20} was incorporated into mixtures of di(Br_2C18:0)PC and di(C18:1)PA (○, △), or di(Br_2C18:0)PA and di(C18:1)PC (□) in 20 mM Hepes, 1 mM EGTA (○, □) or in 20 mM Hepes, 1 mM EGTA, 300 mM KCl (△) at pH 7.2. Fluorescence intensities are expressed as a fraction of that for the peptide in 100% nonbrominated lipid. The molar ratio of phospholipid to protein was 100:1. The solid lines show best fits of the data to eqs 2−4 with the relative binding constants given in Table 2.

Table 2: Relative Binding Constants for Anionic Phospholipids

		relative binding constant[a]	
peptide	system	low salt	high salt
Y_2L_{20}	di(Br_2C18:0)PC−di(C18:0)PA	2.24 ± 0.29	1.64 ± 0.32
	di(Br_2C18:0)PA−di(C18:0)PC	2.58 ± 0.14	1.79 ± 0.39
	di(Br_2C18:0)PC−di(C18:0)PS	1.68 ± 0.19	1.48 ± 0.27
	di(Br_2C18:0)PS−di(C18:0)PC	1.98 ± 0.55	1.40 ± 0.39
Y_2L_{14}	di(Br_2C18:0)PC−di(C18:0)PS	1.79 ±.35	1.44 ± 0.33
	di(Br_2C18:0)PS−di(C18:0)PC	2.04 ± 0.5	1.84 ± 0.39

[a] Binding constant for anionic phospholipid, relative to di(C18:1)PC, calculated from eqs 2−4 with values for *n* of 2.8 and 2.4 for Y_2L_{14} and Y_2L_{20}, respectively.

Effects of Anionic Phospholipids. Fluorescence quenching in mixtures of di(Br_2C18:0)PA and di(C18:1)PA or in mixtures of di(Br_2C18:0)PS and di(C18:1)PS fit to the same values for *n* as in mixtures of di(Br_2C18:0)PC and di(C18:1)PC. Fluorescence quenching for Y_2L_{20} in mixtures of di(C18:1)PA and di(Br_2C18:0)PC is compared to that in mixtures of di(Br_2C18:0)PA and di(C18:1)PC in Figure 7. The more extensive quenching observed at intermediate mole fractions of the brominated component when the brominated component is phosphatidic acid rather than phosphatidylcholine indicates stronger binding of phosphatidic acid to the peptide than phosphatidylcholine. The data were fitted to eqs 2−4 giving the relative binding constants in Table 2. The observation that the relative binding constant obtained when the brominated component is di(Br_2C18:0)PA agrees within experimental error with that obtained when the brominated component is di(Br_2C18:0)PC suggests that all *n* "sites" around the peptide are equivalent, since, for example, strong binding of phosphatidic acid at a small number of sites would have resulted in stronger quenching by di(Br_2C18:0)PA than expected from the ability of di(C18:1)PA to displace di(Br_2C18:0)PC. Effects of ionic strength are relatively small (Figure 7, Table 2).

Relative binding constants for phosphatidylserine determined in mixtures of di(Br_2C18:0)PS and di(C18:1)PC or in mixtures of di(C18:1)PS and di(Br_2C18:0)PC are equal and slightly less than those observed for phosphatidic acid (Table 2). Binding constants for phosphatidylserine with Y_2L_{14} are equal to those for Y_2L_{20}.

DISCUSSION

Effects of Lipid Chain Lengths. The results obtained here show that aromatic residues at the ends of hydrophobic α-helices have a large effect on their interaction with lipid bilayers. In previous studies with the peptides L_{16} and L_{22}, we showed the importance of the relationship between the hydrophobic length of the peptide and the hydrophobic thickness of the lipid bilayer (*3*). The hydrophobic length of the peptide L_{16} is about 27 Å, calculated for a stretch of 18 hydrophobic residues in total, with a helix translation of 1.5 Å/residue; the hydrophobic length of L_{22} calculated in the same way is ca. 36 Å. When the hydrophobic length of the peptide is greater than the hydrophobic thickness of the bilayer, the peptide incorporates into the lipid bilayer, matching between the peptide and the lipid presumably being achieved by tilting of the long axis of the helix with respect to the bilayer normal. However, when the hydrophobic thickness of the bilayer is greater than the hydrophobic length of the peptide by ca. 6 Å or more, the peptide fails to incorporate into the bilayer, forming instead aggregates of peptide separate from the bilayer (*3*); Ren et al. (*5*) obtained very similar results, except that under their conditions, unincorporated peptide bound to the surface of the lipid bilayer, with the long axis of the peptide parallel to the surface.

In contrast to the results with L_{16}, F_2L_{14} incorporated fully into bilayers of di(C24:1)PC (Figure 1). Partitioning of Y_2L_{14} into di(C24:1)PC was less favorable than F_2L_{14} while being more favorable than L_{16}; at a peptide:lipid molar ratio of 1:100, the fluorescence intensity of Y_2L_{14} in di(C24:1)PC was less than in di(C18:1)PC, suggesting only partial incorporation into the bilayer. Increasing the molar ratio of lipid:peptide in the range 50:1 to 400:1 leads to increased fluorescence intensity for Y_2L_{14} (Figure 1B), whereas for L_{16}, full incorporation into lipid bilayers was observed at molar ratios of lipid:peptide greater than 15:1 (*3*). The value of λ_{max} for Y_2L_{14} in di(C24:1)PC shifted only from 317.7 to 315.6 nm with increasing molar ratio of lipid:peptide from 50:1 to 400:1, despite the 2.5-fold increase in fluorescence intensity (Figure 1B). This suggests that the peptide simply equilibrates between an almost nonfluorescent state in water and a fluorescent state spanning the lipid bilayer. On the basis of the measurements of fluorescence intensity, Y_2L_{14} is 50% incorporated into di(C24:1)PC at a molar ratio of lipid:peptide of 75:1, under the experimental conditions used here. This is unlikely to represent a true equilibrium distribution, although comparable results were obtained when peptide was reconstituted into lipid bilayers by mixing lipid and peptide in solution in ethanol followed by dilution into excess buffer, using the procedure described by Ren et al. (*4*, *5*) (unpublished observations).

Values for λ_{max} for the peptides incorporated into lipid bilayers vary little with fatty acyl chain length (Figure 2A) and do not approach the value of λ_{max} for Trp exposed to water, which is about 350 nm (*21*). These experiments, therefore, suggest that the peptides all incorporate into the bilayer in the same way, spanning the bilayer with the Trp residue located toward the middle. For energetic reasons, the only other likely orientation for a bound peptide is one with the long axis of the α-helical peptide running parallel to the bilayer surface, locating the Trp residue at the lipid-water interface (*23*); the very small shifts in λ_{max} with bilayer

thickness suggest that such an orientation is not adopted even in the thickest bilayers.

A fluorescence quenching method was used to obtain binding constants for phosphatidylcholines to the peptides, measured relative to the binding constant for di(C18:1)PC (Table 1). For the peptides L_{16} and L_{22}, strongest binding has been shown to occur when the hydrophobic length of the peptide matches the hydrophobic thickness of the bilayer; strongest binding for L_{16} is to di(C16:1)PC or di(C18:1)PC whereas strongest binding of L_{22} is to di(C22:1)PC (*3*). The effective hydrophobic length of the peptide Y_2L_{14} might be expected to be somewhat greater than that of L_{16}; if the peptide is modeled as an α-helix with the two Tyr residues oriented to be roughly parallel to the long axis of the α-helix, the distance between the two Tyr−OH groups is ca. 33 Å, about 6 Å greater than the hydrophobic length of L_{16}. The hydrophobic length of Y_2L_{14} calculated in this way matches the hydrophobic thickness of a bilayer of di(C20:1)PC, whereas the relative lipid binding constants increase from di(C14:1)PC to di(C22:1)PC (Table 1). Similarly, relative binding constants for F_2L_{14} increase with increasing chain length from di(C14:1)PC to di(C24:1)PC. Analyzing the data in terms of a quenching circle model (eq 6) rather than a lattice model (eqs 2−4) gives the same result, with the constant describing the partitioning of a lipid from the bulk lipid phase into the quenching circle around the peptide increasing ca. 4-fold from di(C14:1)PC to di(C24:1)PC (Table 1).

The results with Y_2L_{14} and F_2L_{14} show that introduction of aromatic residues at the two ends of the hydrophobic sequence increase the ability of the short peptides to partition into thick lipid bilayers. Values for λ_{max} for Y_2L_{14} and F_2L_{14} change little with fatty acyl chain length (Figure 2), suggesting that the environment of the Trp residue changes little with bilayer thickness. The observation that the highest relative binding constant is obtained with bilayers considerably thicker than the calculated hydrophobic length of the peptides suggests that the presence of aromatic residues at the ends of the helices leads to marked thinning of the bilayer around the peptides when the bilayer is much thicker than the hydrophobic length of the peptide. A molecular dynamics simulation of a lipid bilayer containing gramicidin shows considerable distortion of fatty acyl chains around the aromatic residues on gramicidin with the chains "tucking under" the aromatic residues (*24*). However, both experiment (*25*) and theory (*26*) suggest that bilayer thickness is little affected when the bilayer thickness nearly matches the hydrophobic length of the peptide.

The chain length dependence of lipid binding to Y_2L_{20} is much less marked than for the shorter peptides; the relative binding constant increases from di(C14:1)PC to di(C18:1)-PC, but then hardly changes with increasing chain length between di(C18:1)PC and di(C24:)PC (Table 1). This contrasts with L_{22}, which shows markedly stronger interaction with di(C22:1)PC than with phospholipids with shorter or longer chains (*3*). This again suggests that the introduction of the two Tyr residues leads to an increase in the thickness of the bilayer with which optimal interaction of the peptide is observed.

Effects of Lipid Charge. Both phosphatidylserine and phosphatidic acid bind more strongly to the peptides than phosphatidylcholine, the effect of anionic phospholipid decreasing slightly with increasing ionic strength (Table 2). Previous experiments with L_{16} in mixtures of anionic phospholipid and phosphatidylcholine were consistent with the presence on the peptide of a small number of high affinity sites for the anionic phospholipid, together with a large number of sites showing little selectivity between anionic and zwitterionic phospholipids (*6*). This is consistent with a model in which one anionic phospholipid molecule binds closely to the Lys residues at each end of the helix, effectively eliminating the effects of charge on the interaction of subsequent phospholipid molecules. In contrast, quenching profiles for Y_2L_{14} and Y_2L_{20} (Figure 7) show that all *n* sites around the peptide have the same relative binding constant for anionic phospholipid, suggesting that the presence of the Tyr residues prevents close association of the anionic phospholipid group with the cationic Lys residues.

Effects of charge on the interactions between anionic phospholipids and membrane proteins have been shown to be relatively small. The binding constants for phosphatidylserine and phosphatidylcholine for the Ca^{2+}-ATPase have been shown to be the same (*16*). For the Na^+,K^+-ATPase, the binding constant for phosphatidylserine has been shown to be about twice that for phosphatidylcholine, the difference between the two decreasing with increasing ionic strength (*27*).

Effects of Gel Phase Lipid. The spectra shown in Figure 4 show that the peptides incorporate into bilayers of phospholipid in the gel phase. Bilayers of mixtures of di-(C16:0)PC and di(Br_2C18:0)PC are in a two-phase region of the phase diagram at 25 °C, containing separate domains enriched in di(16:0)PC and in di(Br_2C18:0)PC respectively (*16*, *28*). The more marked quenching observed in mixtures of di(C16:0)PC and di(Br_2C18:0)PC than in mixtures of di-(C18:1)PC and di(Br_2C18:0)PC shows that the peptide partitions preferentially into domains of liquid crystalline lipid (Figure 5). The binding constants of L_{16} and Y_2L_{14} for di(C16:0)PC in the gel phase relative to di(C18:1)PC in the liquid crystalline phase are ca. 0.15 (Figure 5), and very similar results are obtained with L_{22} and Y_2L_{20} (data not shown). Thus, the presence of bulky aromatic residues does not have any significant effect on the selectivity for liquid crystalline over gel phase lipid. Further, since Y_2L_{14} shows a preference for longer chain phospholipids than L_{16}, Y_2L_{14} might have been expected to show a greater preference for gel phase lipid than L_{16}, since phospholipid in the gel phase gives a thicker bilayer than the corresponding lipid in the liquid crystalline phase. Since Y_2L_{14} and L_{16} show equal preferences for liquid crystalline over gel phase lipid, this shows that any effects of hydrophobic matching between the peptide and the bilayer are small compared to effects of lipid phase on the interaction energies between the peptides and the lipid. Preferential partitioning of proteins from domains in the gel phase into domains of liquid crystalline lipid has been demonstrated previously for a variety of membrane proteins including bacteriorhodopsin (*29*) and the Ca^{2+}-ATPase (*16*, *30*, *31*).

Quenching in mixtures of sphingomyelin and di(Br_2C18:0)PC at 25 °C is very similar to that observed with mixtures of di(C16:0)PC and di(Br_2C18:0)PC (Figure 5). Mixtures of bovine brain sphingomyelin and di(C18:1)PC will also be in a two-phase region at 25 °C with gel phase domains enriched in sphingomyelin (*22*). Thus, partitioning of the

peptides between gel and liquid crystalline phase lipid shows little dependence on the structure of the phospholipid. It has been suggested that plasma membranes of mammalian cells contain domains or "rafts" enriched in sphingomyelin and that particular enzymes, particularly those associated with cell signaling, are concentrated within the rafts (*32*). The results presented here suggest that membrane proteins containing transmembrane α-helices will tend to be excluded from these rafts, and it may therefore be significant that many of the signaling proteins suggested to be contained within the rafts are anchored to the membrane by GPI anchors (*33*).

Effects of Cholesterol. Addition of cholesterol to bilayers of di(C18:1)PC was found to decrease the partitioning of L_{16} into the bilayers, an effect suggested to follow from an increase in bilayer thickness on addition of cholesterol (*1*). Addition of cholesterol had no significant effect on the partitioning of F_2L_{14} or Y_2L_{14} into di(C18:1)PC (Figure 7), consistent with the observed preference of these peptides for long-chain phospholipids (Table 1). Thus, the presence of Tyr or Phe residues at the ends of the transmembrane α-helices buffers the helices against any bilayer-thickening effects of cholesterol.

Summary. The presence of aromatic residues at the ends of transmembrane α-helices has a marked effect on their interactions with phospholipids, effectively buffering them against changes in bilayer thickness caused either by an increase in the chain length of the phospholipids or by the presence of cholesterol. The presence of aromatic residues at the ends of the helices can also reduce the strength of the charge interaction with anionic phospholipids, although it has no significant effect on the relative preference for domains of liquid crystalline over gel phase lipid. Aromatic residues are commonly found at the ends of transmembrane α-helices in membrane proteins (*12*). The presence of aromatic residues at the ends of transmembrane helices has been shown to be important for the proper function of membrane proteins. For example, in the Ca^{2+}-ATPase mutation of the prominent cluster of aromatic residues at the end of helix M7 leads to an enzyme that can be phosphorylated by ATP, but for which the rate of dephosphorylation is very slow (*34*). Such experiments suggest that the presence of aromatic residues is important for the correct packing of transmembrane α-helices into lipid bilayers.

It has been suggested that the correct matching of the hydrophobic length of a transmembrane α-helix to the thickness of the lipid bilayer is important in the retention of proteins in the Golgi and endoplasmic reticulum membranes (*35*−*37*). Experiments with the simple L_{16} and L_{22} were consistent with such a proposal since the shortest peptide (L_{16}) was found not to incorporate into thick bilayers (*3*). The experiments reported here suggest that such a simple model for retention may not work when the transmembrane region contains aromatic residues at both ends of the transmembrane stretch.

REFERENCES

1. Nezil, F. A., and Bloom, M. (1992) *Biophys. J. 61*, 1176−1183.
2. Huschilt, J. C., Millman, B. M., and Davis, J. H. (1989) *Biochim. Biophys. Acta 979*, 139−141.
3. Webb, R. J., East, J. M., Sharma, R. P., and Lee, A. G. (1998) *Biochemistry 37*, 673−679.
4. Ren, J., Lew, S., Wang, Z., and London, E. (1997) *Biochemistry 36*, 19213−10220.
5. Ren, J., Lew, S., Wang, J., and London, E. (1999) *Biochemistry 38*, 5905−5912.
6. Mall, S., Sharma, R. P., East, J. M., and Lee, A. G. (1999) *Faraday Discuss. 111*, 127−136.
7. Doyle, D. A., Cabral, J. M., Pfuetzner, R. A., Kuo, A., Gulbis, J. M., Cohen, S. L., Chait, B. T., and Mackinnon, R. (1998) *Science 280*, 69−77.
8. Caffrey, M., and Feigenson, G. W. (1981) *Biochemistry 20*, 1949−1961.
9. Johannsson, A., Keightley, C. A., Smith, G. A., Richards, C. D., Hesketh, T. R., and Metcalfe, J. C. (1981) *J. Biol. Chem. 256*, 1643−1650.
10. Starling, A. P., East, J. M., and Lee, A. G. (1993) *Biochemistry 32*, 1593−1600.
11. Lee, A. G. (1998) *Biochim. Biophys. Acta 1376*, 381−390.
12. Landolt-Marticorena, C., Williams, K. A., Deber, C. M., and Reithmeier, R. A. F. (1993) *J. Mol. Biol. 229*, 602−608.
13. Rees, D. C., Chirino, A. J., Kim, K. H., and Komiya, H. (1994) in *Membrane Protein Structure* (White, S. H., Ed.) pp 3−26, OUP, New York.
14. Wimley, W. C., and White, S. H. (1996) *Nat. Struct. Biol. 3*, 842−848.
15. Bolen, E., and Holloway, P. (1990) *Biochemistry 29*, 9638−9643.
16. East, J. M., and Lee, A. G. (1982) *Biochemistry 21*, 4144−4151.
17. Atherton, E., and Sheppard, R. C. (1989) *Solid-phase peptide synthesis: a practical approach*, IRL Press, Oxford.
18. Rooney, E. K., and Lee, A. G. (1986) *J. Biochem. Biophys. Methods 120*, 175−189.
19. East, J. M., Melville, D., and Lee, A. G. (1985) *Biochemistry 24*, 2615−2623.
20. London, E., and Feigenson, G. W. (1981) *Biochemistry 20*, 1932−1938.
21. Lakowicz, J. R. (1983) *Principles of Fluorescence Spectroscopy*, Plenum Press, New York.
22. Untracht, S. M., and Shipley, G. G. (1977) *J. Biol. Chem 252*, 4449−4457.
23. White, S. H., and Wimley, W. C. (1999) *Annu. Rev. Biophys. Biomol. Struct. 28*, 319−365.
24. Woolf, T. B., and Roux, B. (1996) *Proteins: Struct., Funct., Genet. 24*, 92−114.
25. de Planque, M. R. R., Greathouse, D. V., Koeppe, R. E., Schafer, H., Marsh, D., and Killian, J. A. (1998) *Biochemistry 37*, 9333−9345.
26. Tieleman, D. P., Forrest, L. S., Sansom, M. S. P., and Berendsen, H. J. C. (1998) *Biochemistry 37*, 17554−17561.
27. Esmann, M., and Marsh, D. (1985) *Biochemistry 24*, 3572−3578.
28. Lee, A. G. (1977) *Biochim. Biophys. Acta 472*, 285−344.
29. Cherry, R. J., Muller, U., Henderson, R., and Heyn, M. P. (1978) *J. Mol. Biol. 121*, 283−298.
30. London, E., and Feigenson, G. W. (1981) *Biochemistry 20*, 1939−1948.
31. Kleeman, W., and McConnell, H. M. (1976) *Biochim. Biophys. Acta 419*, 206−222.
32. Simons, K., and Ikonen, E. (1997) *Nature 387*, 569−572.
33. Harder, T., and Simons, K. (1997) *Curr. Opin. Cell Biol. 9*, 534−542.
34. Adams, P., East, J. M., Lee, A. G., and O'Connor, C. D. (1998) *Biochem. J. 335*, 131−138.
35. Bretscher, M. S., and Munro, S. (1993) *Science 261*, 1280−1281.
36. Masibay, A. S., Balaji, P. V., Boeggeman, E. F., and Qasba, P. K. (1993) *J. Biol. Chem. 268*, 9908−9916.
37. Pedrazzini, E., Villa, A., and Borgese, N. (1996) *Proc. Natl. Acad. Sci. U.S.A. 93*, 4207−4212.
38. Lewis, B. A., and Engelman, D. M. (1983) *J. Mol. Biol. 166*, 211−217.
39. Sperotto, M. M., and Mouritsen, O. G. (1988) *Eur. Biophys. J. 16*, 1−10.

BI992205U